Redox Biology 28 (2020) 101354

Contents lists available at ScienceDirect

Redox Biology

journal homepage: www.elsevier.com/locate/redox

Inducible nitric oxide synthase-derived extracellular nitric oxide flux regulates proinflammatory responses at the single cell level

Veena Somasundaram[a], Anne C. Gilmore[b], Debashree Basudhar[a], Erika Mariana Palmieri[a], David A. Scheiblin[c], William F. Heinz[c], Robert.Y.S. Cheng[a], Lisa A. Ridnour[a], Grégoire Altan-Bonnet[a], Stephen J. Lockett[c], Daniel W. McVicar[a], David A. Wink[a,*]

[a] Cancer and Inflammation Program, Center for Cancer Research, National Cancer Institute, National Institute of Health, USA
[b] Optical Microscopy and Analysis Laboratory, Office of Science and Technology Resources, Center for Cancer Research, National Cancer Institute, USA
[c] Optical Microscopy and Analysis Laboratory, Cancer Research Technology Program, Frederick National Laboratory for Cancer Research, Frederick, MD, USA

ARTICLE INFO

Keywords:
Nos2
Macrophage
Tumor
Metabolism

ABSTRACT

The role of nitric oxide (NO) in cancer progression has largely been studied in the context of tumor NOS2 expression. However, pro- versus anti-tumor signaling is also affected by tumor cell-macrophage interactions. While these cell-cell interactions are partly regulated by NO, the functional effects of NO flux on proinflammatory (M1) macrophages are unknown. Using a triple negative murine breast cancer model, we explored the potential role of macrophage Nos2 on 4T1 tumor progression. The effects of NO on macrophage phenotype were examined in bone marrow derived macrophages from wild type and $Nos2^{-/-}$ mice following *in vitro* stimulation with cytokine/LPS combinations to produce low, medium, and high NO flux. Remarkably, Nos2 induction was spatially distinct, where $Nos2^{high}$ cells expressed low cyclooxygenase-2 (Cox2) and vice versa. Importantly, *in vitro* M1 polarization with IFNγ + LPS induced high NO flux that was restricted to cells harboring depolarized mitochondria. This flux altered the magnitude and spatial extent of hypoxic gradients. Metabolic and single cell analyses demonstrated that single cell Nos2 induction limited the generation of hypoxic gradients *in vitro*, and Nos2-dependent and independent features may collaborate to regulate M1 functionality. It was found that Cox2 expression was important for $Nos2^{high}$ cells to maintain NO tolerance. Furthermore, Nos2 and Cox2 expression in 4T1 mouse tumors was spatially orthogonal forming distinct cellular neighborhoods. In summary, the location and type of $Nos2^{high}$ cells, NO flux, and the inflammatory status of other cells, such as $Cox2^{high}$ cells in the tumor niche contribute to Nos2 inflammatory mechanisms that promote disease progression of 4T1 tumors.

1. Introduction

Historically, NO flux from murine macrophages was thought to be in the anti-tumor, anti-angiogenic and anti-pathogen range (> 500 nM), but more recently, lower levels (< 500 nM) were found to be critical in wound healing responses exploited by the tumor during disease progression [1–4]. Early studies have shown that exposure of ANA-1 macrophages to different M1-polarizing cytokine combinations generated different NO flux. Because NO effects are concentration dependent, these results implicated stimulus-specific biological ramifications of NO produced by macrophages [5]. Importantly, this range of NO flux can be produced by cytokine-stimulated macrophages in the tumor microenvironment (TME) [6]. High levels of NO induce apoptosis in leukemic cells in murine models as well as necrosis in glioblastoma multiforme in humans, but high expression of NOS2 and co-expression with COX2 is associated with poor prognosis in Estrogen Receptor negative (ER-) breast cancer patients [1,2,7–9]. Previous studies have examined the expression of NOS2 and COX2 within the tumor and the downstream effects of high versus low expression of these proteins within tumor cells [8]. In addition to tumor cell signaling, Nos2 elicits specific effects within the host immune compartment. Toward this end, immunosuppressive effects of NO have been reported, involving T cell inhibition through increased IL-10 and TGFβ, thus reducing therapeutic efficacy [10,11,49]. In contrast, $Nos2^{high}$ macrophages have been shown to increase trafficking of CD8 cytolytic T cells and myeloid cells [12,13] to regions affected by focussed irradiation or cytosine-phosphorothioate-guanine oligodeoxynucleotide (CpG-ODN) applications, suggesting both spatially- and temporally-

* Corresponding author. Cancer and Inflammation Program, National Cancer Institute, NIH, Frederick, MD, 21702, NCI-Frederick, USA.
E-mail address: wink@mail.nih.gov (D.A. Wink).

https://doi.org/10.1016/j.redox.2019.101354
Received 6 September 2019; Received in revised form 4 October 2019; Accepted 18 October 2019
Available online 01 November 2019

dependent 'push-pull' type of mechanisms where increased CD8 cytolytic activity could then be limited by IL-10 induction. As localized NO flux within the TME can determine the fate of the tumor, NOS2 expression by immune cells provides an important target for improved therapeutic efficacy. Therefore, our current understanding of these processes can be improved by exploring the mechanistic impact of host Nos2-derived NO levels within the TME in murine tumor models.

We previously showed that NOS2-derived NO contributes to the aggressive phenotype of invasive ER negative (ER-) MDA-MB-231 xenografts, which is mediated at least in part by NO feed-forward mechanisms that up-regulate NOS2, COX2, TLR agonist S100A8, and inflammatory cytokines IL-6 and IL-8 [1,2]. More recently, we showed that elevated tumor expression of both NOS2 and COX2 strongly predicted poor disease specific survival in ER- breast cancer patients while the dual inhibition of these enzymes reduced primary tumor growth of MDA-MB-231 xenografts [8].

In the current study, we show that $Nos2^{-/-}$ mice have considerably decreased metastatic burden implicating the host Nos2 in tumor progression. Furthermore, we show that low flux NO increases migration in 4T1, murine mammary tumor cells, while higher flux limits motility and causes cytostasis. Thus, the level of NO and proximity to the NO source will impact these functional effects. We show that different cytokine/LPS stimuli activate macrophage cell lines and BMDMs (from WT and $Nos2^{-/-}$ mice) to produce different NO flux. We find that NO flux is dependent on both the Nos2 expression in individual cells and more importantly the density of Nos2 expressing cells. This suggests that higher density of Nos2 expressing cells leads to higher NO flux which impacts morphology as well oxygen consumption within the TME. Furthermore, we illustrate the importance of the synergy between Cox2 and Nos2 in regulating inflammation and demonstrate that high Nos2 and high Cox2 expressing cells are spatially separated and support one another in a paracrine fashion. These results suggest that at the single cell level, $Nos2^{high}$ and $Cox2^{high}$ cells act in trans to affect metabolic changes within neighboring cells in the TME that tunes the inflammatory microenvironment.

2. Results

2.1. Host Nos2 promotes pulmonary metastasis of aggressive breast cancers

Previous studies showed that elevated tumor NOS2 expression predicted poor survival in patients with ER- breast cancer and that NO flux equivalent to that produced by ~300 μM DETA/NO could drive a feed-forward signaling loop, which promoted disease progression [1,2]. Pharmacological inhibition of NOS2 and COX2 significantly reduced ER- breast tumor growth in nude mice [1,7,8]. Importantly, pharmacological inhibition affects both tumor and host NOS2 and COX2. Herein, we attempt to delineate a functional role of host Nos2-derived NO in breast tumor progression using 4T1 tumor-bearing mice, a murine model for triple negative breast cancer (TNBC) where metastatic disease develops spontaneously from the primary tumor, and progressively spreads to lymph nodes, lung, and liver similar to human disease [14]. The 4T1 triple negative murine syngeneic model is a suitable model for comparison to human disease as metastatic lesions develop spontaneously from the primary tumor, and the progressive spread to lymph nodes, lung, and liver is very similar to that of human disease [15,16]. Indeed, 4T1 cells exhibited an increased migratory potential *in vitro* with increasing doses of exogenous NO generated by the NO donor DETA/NO at concentrations up to 100 μM (Fig. 1A and B) while at higher doses (1000 μM) the motility was reduced. These results suggest that extracellular NO produced in the TME by macrophages could promote tumor cell migration. Many molecules in the inflammatory microenvironment regulate Nos2 expression. Our recent work showed that COX2, via its product prostaglandin E2 (PGE2), is one important regulator of NOS2 expression in human breast cancer [8]. To explore potential Nos2/Cox2 roles in disease progression, tumor growth, and lung metastatic burden was examined in 4T1 tumor-bearing WT and $Nos2^{-/-}$ mice treated with or without the COX inhibitor indomethacin. Lung metastatic burden was significantly reduced in $Nos2^{-/-}$ mice while indomethacin slowed growth of the primary lesion. This effect was augmented in $Nos2^{-/-}$ mice (Fig. 1C and D). Because indomethacin treated mice survived longer due to delayed tumor growth, more metastatic lesions were visible, however the number of metastases were not significantly different in WT and $Nos2^{-/-}$ mice receiving indomethacin. Mechanistically, indomethacin showed anti-proliferative effects directly in 4T1 cells grown *in vitro* over an 83h window at 50 and 100 μM concentrations (Fig. 1E). A trend of increased median survival from 51 days in treated WT mice to 60 days in treated $Nos2^{-/-}$ mice was observed (Fig. 1F). Together, these results suggest that host NO production facilitates 4T1 motility and escape from primary tumor site thereby increasing metastatic lesions. However, effects of different doses of NO are vastly different and as we found a role of host NO in the TME, we sought to further explore the context of this relationship by examining NO production by macrophages under various stimuli that are known to exist in a tumor niche, namely combinations of IFNγ, IL1β, TNFα and TLR4 ligands (LPS).

2.2. Different proinflammatory stimuli induce distinct extracellular NO flux

ANA-1 murine macrophages stimulated with combinations of cytokines/LPS produce different levels of NO characterized by low, intermediate, and high NO flux generated by IFNγ + IL1β, IFNγ + TNFα and IFNγ + LPS, respectively, as visualized by Nos2 protein expression, nitrite levels, and nitrosative capacity (N_2O_3; DAN nitrosation) profiles of stimulated cells (Fig. 2A) [5]. Similar responses were observed in murine bone marrow-derived macrophages (BMDMs) from BALB/c (Fig. 2B) or C57BL/6 (BL6) (Fig. S1A) mice, with the exception that in BMDM, LPS alone (18hr) elicited intermediate NO flux which was markedly augmented when combined with IFNγ. In contrast, IFNγ + TNFα generated lower NO flux. Unlike the BMDMs, RAW264.7 cells, appear to be activated by single treatment with LPS or IFNγ, and NO production is augmented by their combination (Fig. S1A). Thus, the response to cytokine combinations is similar to results previously described in ANA-1 cells [5]. Apart from IFNγ + LPS treatment, Nos2 protein induction profiles induced by 18h cytokine stimulation was less robust in BL6 and BALB/c BMDMs when compared to similarly treated immortalized macrophages (Fig. 2A, Fig. S1A). Time course analyses revealed that Nos2 induction was temporally-regulated based on specific cytokine combinations. Nos2 induction occurred as early as 4h in stimulated ANA-1 (Fig. S1C). In contrast, IFNγ + LPS stimulation of BL6 BMDMs induced Nos2 protein within the 24h window and peaked at 42h (Fig. S1D). Real-time production of N_2O_3 measured by DAN peaked at 24h then modestly decreased at 42h; this result is supported by elevated nitrite levels, which peaked at 42h and is consistent with the Nos2 protein expression profile in response to IFNγ + LPS stimulation (Fig. S1D). IFNγ + TNFα combination induced Nos2 protein, N_2O_3 measured by DAN, and nitrite at 42h (Fig. S1D). In BALB/c BMDMs, IFNγ + TNFα stimulation produced measurable levels of Nos2 protein and nitrite at 24h and 42h and slightly higher nitrosative capacity at 42h (Figs. 2C and S1E). Stimulation with IFNγ + LPS potently induced Nos2/NO, while other cytokine combinations were weaker stimulants and slower inducers of Nos2/NO. Also, citrulline levels (the product of L-arginine oxidation by Nos2) increased consistently with NO flux in WT and not $Nos2^{-/-}$ cell lysates after 42h cytokine stimulation, L-arginine consumption by arginase was negligible (Fig. S1B). Therefore, citrulline can also be employed as a robust intracellular readout of NO flux under these conditions. To further analyze the physiological relevance of macrophage-derived NO flux in cancer progression, we performed transwell experiments to explore the NO-induced migratory potential of 4T1 cells cultured with cytokine-stimulated ANA-1 macrophage. Nitric oxide produced by IFNγ + IL1β or IFNγ + TNFα stimulated ANA-1 cells significantly induced 4T1

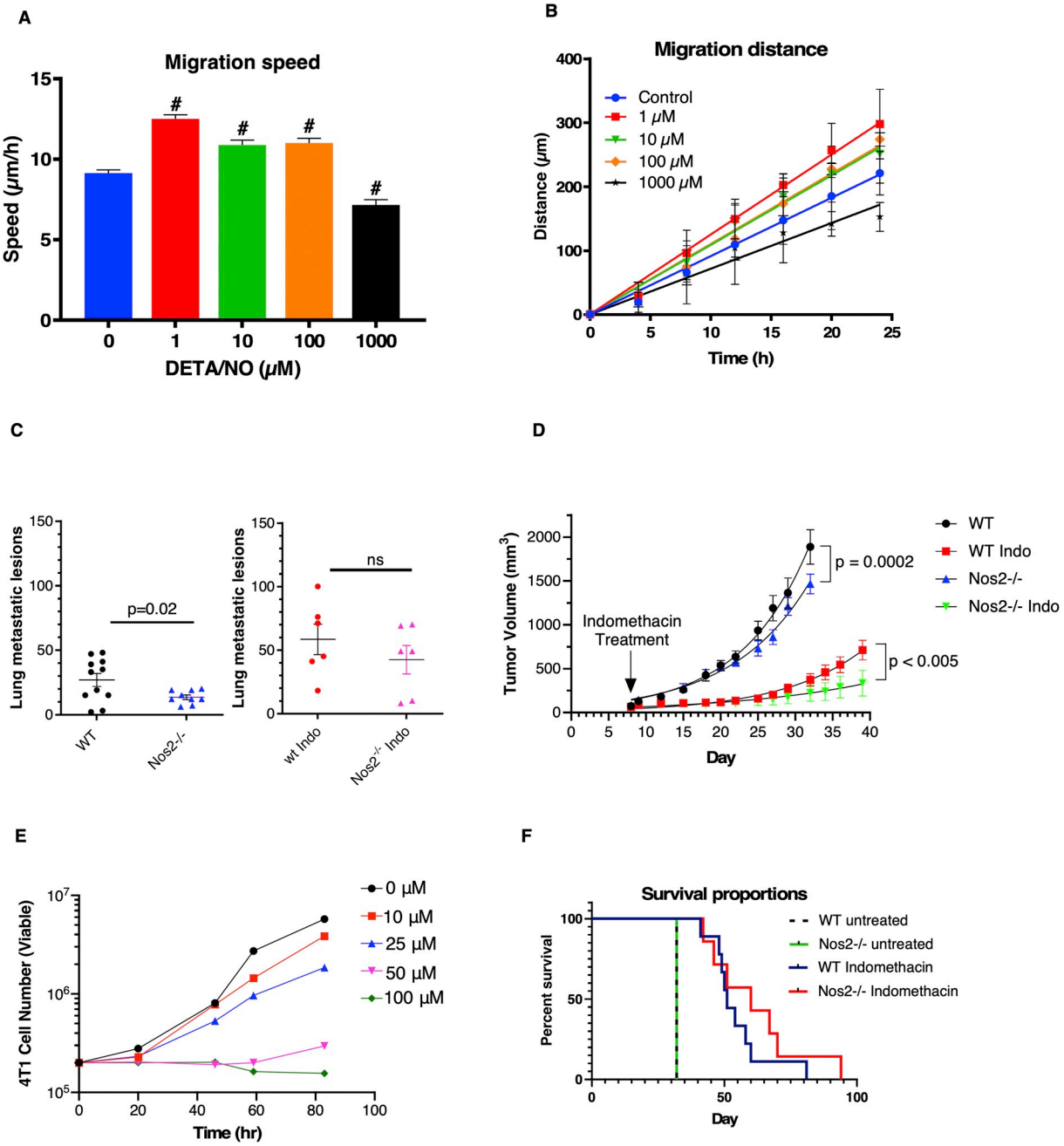

Fig. 1. Migration speed of (A) and distance moved by (B) 4T1 cells treated with varying doses of DETA/NO using *in vitro* migration assay. C. Number of metastatic lesions in the lungs of tumor bearing, WT and Nos2$^{-/-}$ mice that are untreated or treated with 30 mg/L indomethacin (n ≥ 6). D. Tumor volume measurements in WT and Nos2$^{-/-}$ mice that are untreated or treated with 30 mg/L indomethacin (non-linear regression) (n ≥ 6). The untreated tumor bearing mice were euthanized on day 32 when the mice reached tumor limit (2000 mm^3). The indomethacin treated mice were subjected to staggered euthanasia as the tumors reached the permitted size limit of 2000 mm^3 and tumors and lungs were harvested. E. 4T1 viability (trypan blue assay) in presence of varying concentrations of Indomethacin. F. Survival analysis of indomethacin treated, tumor-bearing WT and Nos2−/− mice, (n = 6). (For interpretation of the references to colour in this figure legend, the reader is referred to the Web version of this article.)

migration; in contrast, 4T1 migration in IFNγ + LPS stimulated ANA-1 cocultures was similar to that observed in the presence of unstimulated ANA-1 cells (Fig. 2D, Fig. S1F).

Cellular morphology can be used as an index of inflammatory status as M1 but not M2 macrophages have a flattened morphology [17]. Cytokine stimulated WT cells displayed a flattened M1-like morphology suggesting that Nos2 is required for this phenotype (Fig. 3A). Statistical analysis of altered cellular morphology analyzed using an automated MATLAB algorithm, revealed that stimulated WT BMDMs significantly deviated in shape from unstimulated cells (deviation from Sphericity). This was not observed in Nos2$^{-/-}$ BMDMs that were treated with the same combinations of stimuli (Fig. 3B). These results suggest that intermediate to high Nos2 protein and NO levels are necessary to induce M1-proinflammatory morphology in stimulated macrophages. Despite a 42h stimulation by IFNγ alone or IFNγ + IL1β, cells are unable to reach the highly proinflammatory phenotype induced by IFNγ + LPS in terms of morphological changes or NO production. The persistence of these stimuli within the TME at different stages of disease progression could

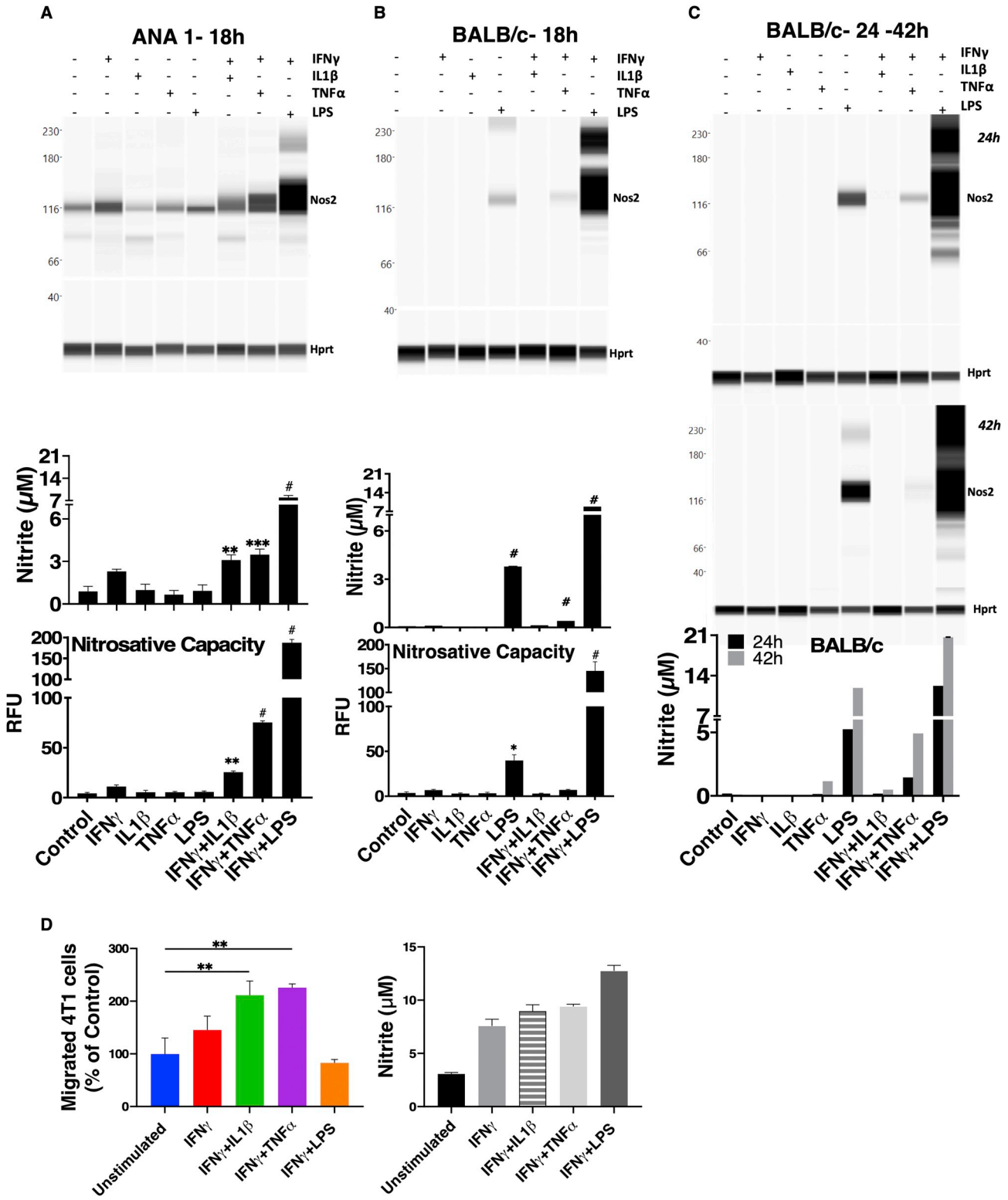

Fig. 2. Extracellular NO flux are entirely dependent on temporally regulated Nos2 expression and correlate with intracellular citrulline levels. WES (Nos2 protein expression), Griess assay (nitrite levels) [46] and DAN Assay (nitrosative capacity) [45], were performed on ANA-1 cells (A) or BALB/c BMDMs (B) stimulated for 18h. C. Nos2 protein analysis in BALB/c BMDMs stimulated for 24h (top panel) or 42h (middle panel) and Griess assay in BALB/c BMDMs stimulated for 24h and 42h (bottom panel). Error bars show SEM (n ≥ 3). RFU: Relative Fluorescence Units. D. Quantification of the migrated 4T1 cells from transwell assay using 6h stimulated ANA-1 cells in the lower compartment of the chamber (Left panel). Right panel shows the nitrite production by 6h-stimulated ANA-1 cells after the 20h transwell assay.

promote distinct NO-dependent effects. Thus, we have delineated the flux dependent effects of NO in inflammatory macrophages. Previously, in cancer cells, and currently in macrophages, we found a synergy between Cox2 and Nos2 expression. Hence, we further explored the role of host Nos2-derived NO flux gradients on Cox2 expression and downstream metabolic effects within the TME.

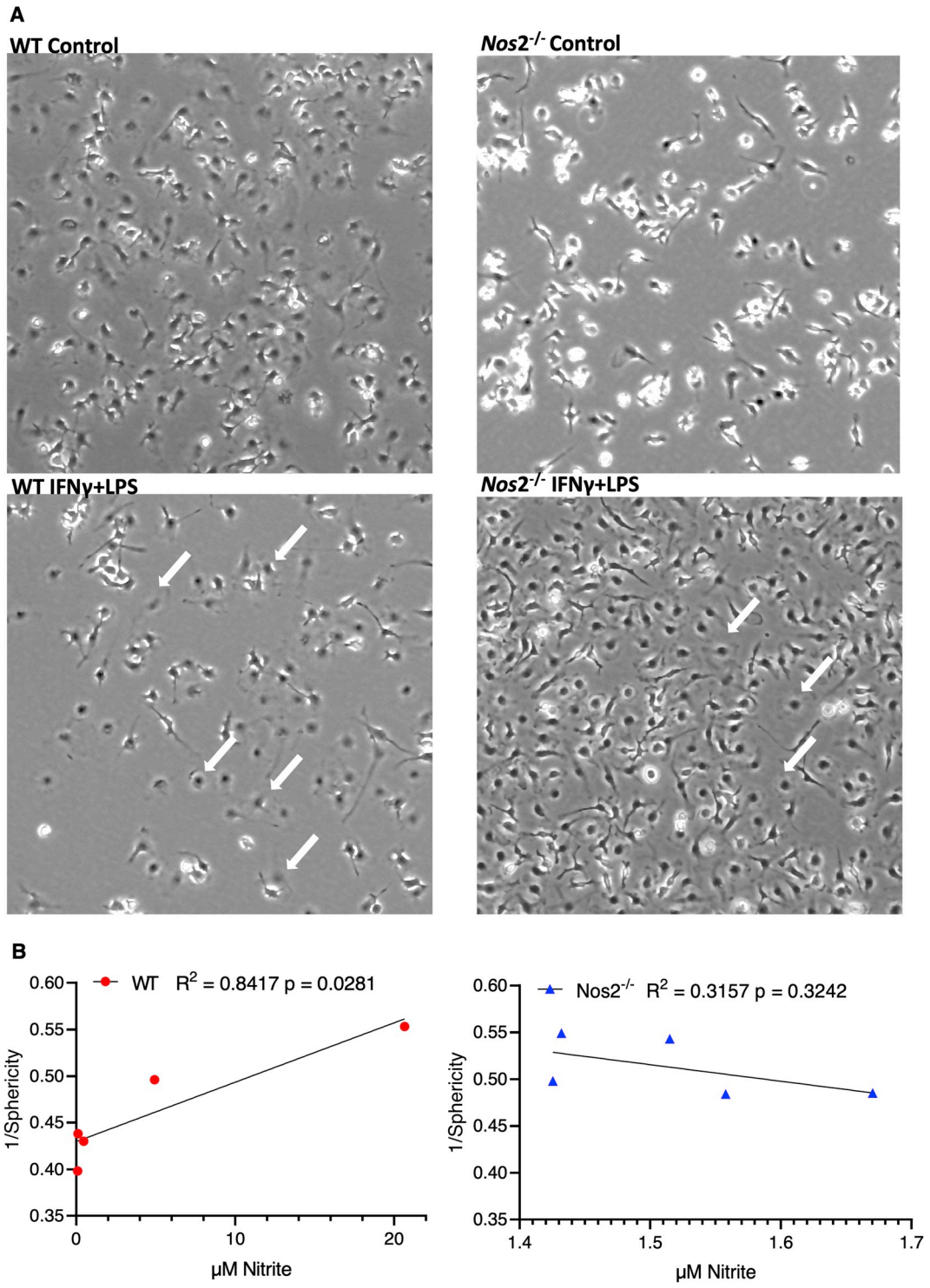

Fig. 3. A. Nos2-derived high NO flux induces 'M1' morphology. Light microscopy images of unstimulated and 42h stimulated WT and Nos2$^{-/-}$ macrophages. Differences in morphology between 'M0' and 'M1' macrophages computed using an automated algorithm to measure the flattening of BMDMs upon 'M1' stimulation. White arrows indicate the cells showing flattened morphology. B. Pearson correlation analysis of flattening (Sphericity^{-1}) and nitrite production by stimulated macrophages shows a significant correlation between reduction in sphericity/increased flattening and increasing nitrite levels. Stimulated Nos2$^{-/-}$ BMDMs do not show this increase in flattening.

2.3. Nos2-Cox2 synergy in inflammation

Inflammatory macrophages have been shown to tolerate prolonged exposure to high NO flux [18]. Given that Cox2 is an important inflammation-associated protein, we examined Nos2 and Cox2 expression in stimulated macrophages in order to investigate a potential Nos2/Cox2 synergy in this effect. Remarkably, we found their expression to be spatially distinct; Nos2^{high} cells were always Cox2^{low} (Figs. 4A and S2B) and the intensity of Nos2 correlated inversely with that of Cox2 (Figs. 4B, S2A, S2B). Regardless, Cox inhibition by indomethacin abrogated the nitrosative capacity of IFNγ + TNFα and IFNγ + LPS stimulated ANA-1 cells (Fig. 4C) as well as stimulated RAW264.7 cells (Fig. S2C). Conversely, addition of DETA/NO to ANA-1 cells caused a dose-dependent induction of Cox2 with 300 μM DETA/NO eliciting levels of

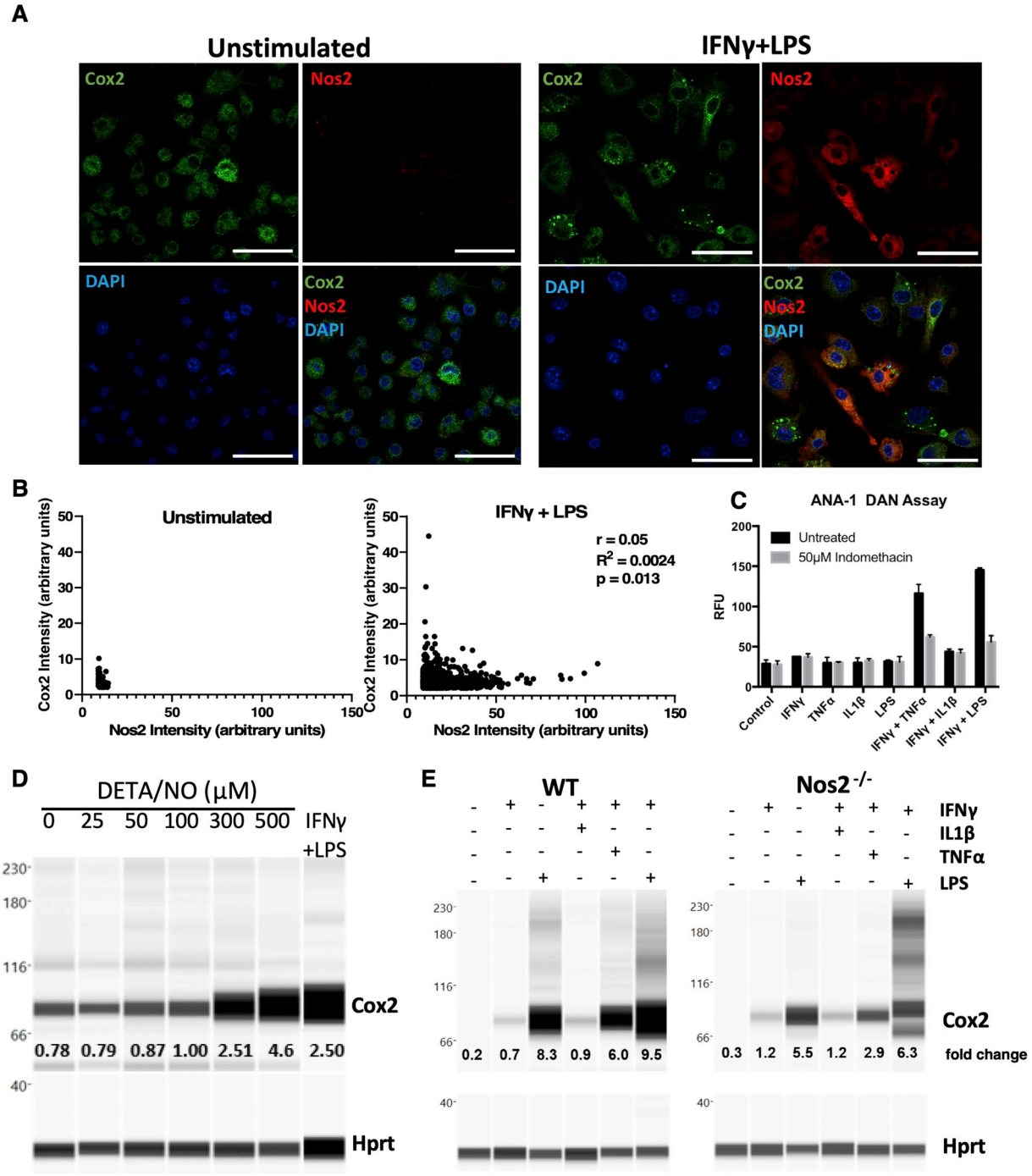

Fig. 4. Nos2-Cox2 synergy in inflammation. A. Nos2 and Cox2 expression in 18h stimulated ANA1 cells analyzed by fluorescent microscopy, scale bar = 50 μm. B: Intensity plots of Nos2 and Cox2 in unstimulated and IFNγ + LPS stimulated cells. C. Nitrosative capacity of stimulated ANA-1 treated with indomethacin. D. WES analysis of Cox2 expression in 24h DETA/NO treated ANA-1 compared to IFNγ + LPS stimulated ANA-1. Fold change in Cox2 protein compared to Hprt with increasing doses of DETA/NO and IFNγ + LPS stimulation are indicated. E. WES in 42h stimulated WT and Nos2$^{-/-}$ BMDMs. Error bars show SEM (n ≥ 3).

Cox2 comparable to IFNγ + LPS stimulation (Fig. 4D). Further, Cox2 induction by combination stimuli was limited in Nos2$^{-/-}$ BMDMs (Fig. 4E) although LPS can induce significant Cox2 expression and PGE2 production in the absence of Nos2, IFNγ + LPS- and IFNγ + TNFα-mediated Cox2 induction is much lower in Nos2$^{-/-}$ cells indicating a role of Nos2-mediated Cox2 induction under these stimuli (Fig. 4E, Fig. S2D). These data suggest Nos2/Cox2 cross-talk regulation in macrophages in a manner similar to that shown in breast cancer cells [8], indicating a critical interplay between these important inflammatory proteins and cell types.

2.4. Nos2 and Cox2 affect a mutual, reciprocal, paracrine regulation in vivo

Elevated NOS2 and COX2 expression is a strong predictor of poor clinical outcome in ER- breast cancer (TNBC) [2,8]. To further explore this relationship within the TME, the spatial organization of Nos2 and Cox2 expression within tumor tissues was examined in 4T1 murine triple negative mammary tumors. In support of our earlier work in human breast cancer cells [1], cytokine stimulated 4T1 murine TNBC cells produce biochemically detectable levels of Nos2 protein and N_2O_3 (Fig. 5A and B). In contrast to macrophages, 4T1 tumor cells showed

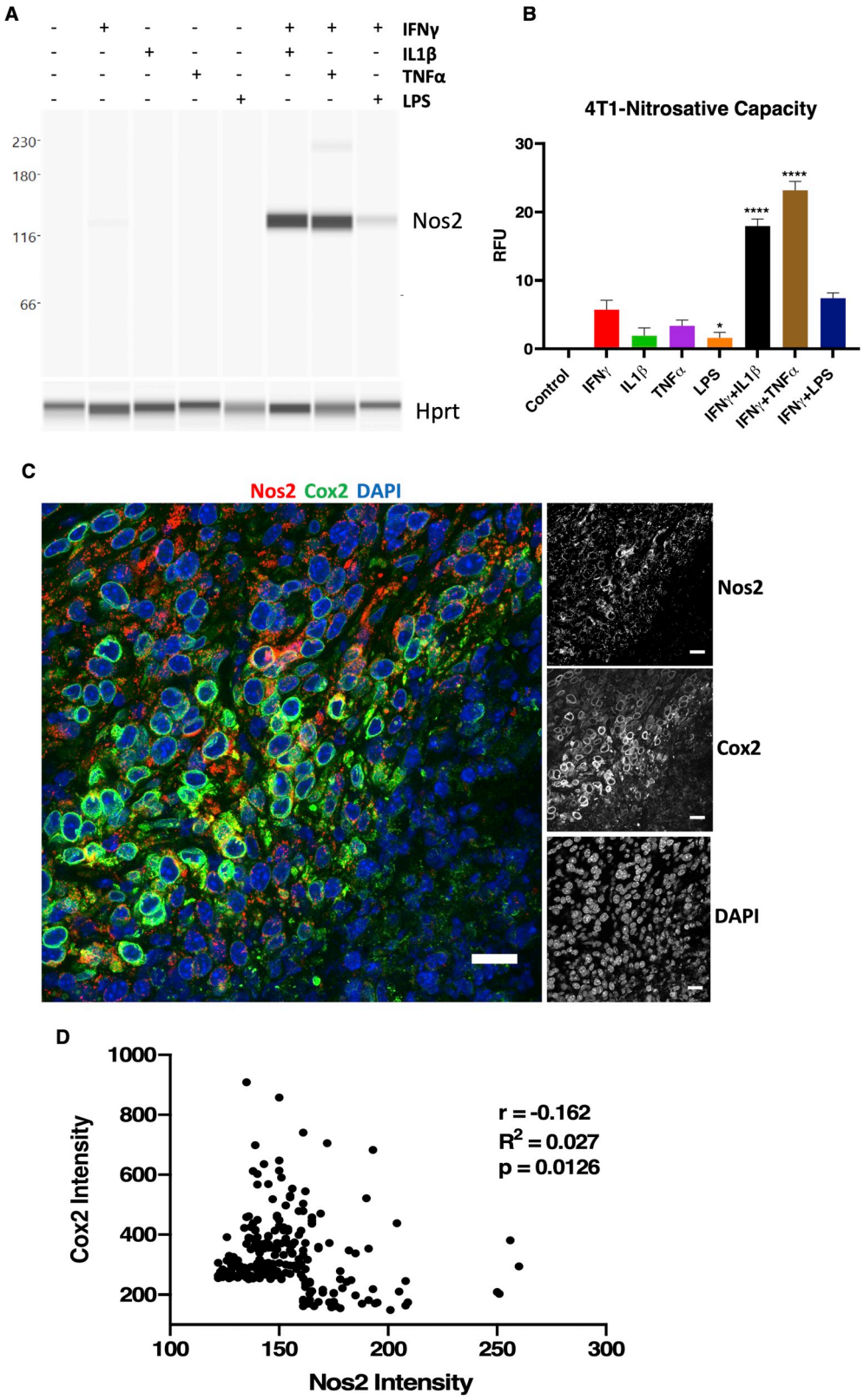

Fig. 5. Nos2 and Cox2 affect a mutual, reciprocal, paracrine regulation *in vivo*. A. Nos2 expression in 24h cytokines/LPS stimulated 4T1 cells. B. In vitro nitrosative capacity of 4T1 cells stimulated for 24h with cytokines/LPS. C. Nos2 and Cox2 expression observed in separate cells in 4T1 tumors. Single channel grayscale images are shown. Scale bar = 20 μm. D. Statistical analysis (Pearson correlation) of Nos2+ and Cox2+ cells based on fluorescence signal intensity.

highest Nos2 induction and N_2O_3 upon stimulation with IFNγ + IL1β or IFNγ + TNFα but were induced less by IFNγ + LPS (Fig. 5A and B). 4T1 cells express basal levels of Cox2, which does not increase appreciably with stimuli (Fig. S6). However, in a manner similar to stimulated macrophages, Nos2 and Cox2 protein expression was spatially distinct and the intracellular expression of these proteins was in general

inversely correlated (Fig. 5C and D). Importantly, the reciprocal regulation of Nos2 and Cox2 by one another is largely a paracrine effect suggesting that the spatial regulation of Nos2 and Cox2 between cells is a mutually synergistic and relevant relationship within the TME. These experiments have also been performed in human breast cancer cells and have shown the same trend of NO production where intermediate levels of NO promote survival and metastasis of human breast tumor cells. This adds credence to the ability of the 4T1 model to recapitulate human breast cancer.

2.5. Effects of NO on oxygen consumption are dependent on NO flux and frequency of Nos2+ cells

One of the important roles of NO is tuning the TME with respect to oxygen and nutrients. In macrophages, high NO flux induced by IFNγ + LPS inhibits oxidative phosphorylation (OXPHOS) and induces glycolytic commitment [19,20]. However, different NO flux promotes distinct metabolic effects at various stages of cancer progression. Therefore, we explored the impact of gradient NO flux on intracellular metabolism. It was recently found that Nos2-derived NO caused a break in the tricarboxylic acid (TCA) cycle by inhibiting the enzyme aconitase 2, which led to an accumulation of intracellular citrate (Unpublished data). Here, we found that stimuli that elicited intermediate levels of NO flux, failed to promote citrate accumulation proving that this occurred only at high NO flux, consistent with those induced by IFNγ + LPS-stimulated BMDMs and was Nos2-dependent as citrate accumulation did not occur in $Nos2^{-/-}$ BMDMs under the same conditions. (Fig. 6A). This is in contrast to lactate production, an indicator of glycolysis. We found increased cellular lactate in both WT and $Nos2^{-/-}$ BMDMs treated with IFNγ + TNFα, and IFNγ + LPS suggesting that cytokines can promote glycolysis independent of Nos2 (Fig. 6B).

The ratio of oxygen consumption rate (OCR) to extracellular acidification rate (ECAR), another readout of mitochondrial metabolism, was inversely proportional to the NO flux in ANA-1 cells treated with IFNγ-combination stimuli (Figs. 6C and S3B). BMDMs exhibited reduced OCR/ECAR in response to high NO flux (Figs. 6D and S3B). In addition, cytokine stimuli potently reduced OCR/ECAR in RAW264.7 and BL6 BMDMs (Figs. S3A and S3B). Cytokine stimulation did not affect OCR in $Nos2^{-/-}$ BMDMs (Figs. S3C and S3D) suggesting that this phenomenon is driven by medium to high Nos2-derived NO flux when compared to the response of stimulated WT BMDMs. For each stimulus, we found that reduction in oxygen consumption was proportional to cell density in WT BMDMs (Fig. S3C). Mitochondrial OCR was significantly reduced upon IFNγ + LPS stimulation irrespective of the plating density. However, the OCR in IFNγ + LPS stimulated cells compared to unstimulated cells was significantly higher when 50,000 cells were stimulated compared to 75,000 and 100,000 (Fig. 6E). This is indicative of a cell density dependent effect of $Nos2^{high}$ cells showing that alterations in the density of NO producing cells effects local NO concentrations and downstream physiologic affects.

2.6. Spatially distinct Nos2 expression affects single-cell redox immunometabolism

The cell density-dependent variability in OXPHOS regulation led us to explore the aspect of heterogeneity that exists *in vivo* in an inflammatory TME. Flow cytometry and microscopic analysis revealed clustered Nos2 expression in cells stimulated *in vitro* with IFNγ + TNFα, which induced intermediate levels of Nos2 while IFNγ + LPS exhibited densely clustered Nos2 in larger regions of the stimulated cells (Fig. 7A and B). In contrast, IFNγ + IL1β induced faint Nos2 in the least number of cells. The median fluorescence intensity (MFI) also followed these same trends. Nos2 expression increased over time in the stimulated single macrophages suggesting an NO-mediated feed-forward mechanism of *Nos2* expression (Fig. 7A), which supports earlier findings in ER- breast cancer cells [1]. Consistent with the known effects of high NO flux on mitochondrial function, statistical analysis of stimulated macrophages stained with the mitochondrial membrane potential dye, tetramethyl rhodamine ethyl ester (TMRE), revealed that Nos2-negative cells had significantly higher TMRE fluorescence implicating increased functional mitochondria when compared to Nos2-positive cells (Fig. 7C and D; Figs. S4A and S4B). Using conditional probability analysis as explained in Table S1, we examined the likelihood of $TMRE^{high}$ cells being $Nos2^{high}$ and found that in IFNγ + LPS stimulated macrophages there was a 19.1% chance of polarized cells possessing high Nos2. This analysis is supported by increased mitochondrial depolarization seen in macrophages treated with 300–500 μM DETA/NO (Fig. S4C). Co-culture experiments with GFP-tagged 4T1 tumor cells and stimulated, Hoechst labelled ANA-1 cells revealed that IFNγ + LPS stimulated ANA-1 cells (blue) could depolarize the mitochondria of the unstimulated 4T1-GFP cells in the co-culture (Fig. 7E). This shows that NO produced by stimulated macrophages can function in trans to affect cellular processes of neighboring cells in the local microenvironment. Next, we explored the physiologic relevance of NO-mediated effects on oxygen consumption and mitochondrial depolarization.

The microenvironment is a key modulator of NO effects, as NO is a diffusible gaseous molecule that reacts quickly with the closest and most chemically reactive molecule within its microenvironment. Oxygen is a key reactant with NO, and impacts redox signaling [21]. We found that tissue hypoxia defined as less than 3% O_2 increased the nitrosative capacity of stimulated macrophages (Fig. 7F, Fig. S4D). NO production has been linked to decreased oxygen consumption in hypoxic environments. We found that only stimulated macrophage will migrate to the hypoxic regions (data not shown), thus suggesting NO may affect pO_2 gradient within the TME. To model the effect of macrophages on tumor hypoxia, we utilized a chamber system for cell culture that forms cell-generated hypoxic and metabolic gradients in two-dimensions (Fig. 7G) – analogous to diffusion between a capillary and nearby tissue [22]. High flux NO generated by IFNγ + LPS stimulated ANA-1 macrophages reduced O_2 consumption within the chamber, thus limiting the generation of a hypoxic gradient defined by the increased distance away from the chamber hole (Fig. 7H). The hypoxic front remained unaffected in stimulated $Nos2^{-/-}$ BMDMs (Fig. S4E) thereby implicating Nos2-derived NO flux as a driver of this phenomenon. Nos2-derived NO from stimulated macrophages reduced mitochondrial membrane potential (Fig. 7E) and O_2 consumption (Fig. 6E and F), in addition to delayed onset of hypoxia in the chamber system. Furthermore, direct blocking of mitochondrial complex I with antimycin A and rotenone was enough to extend the hypoxic front and this was augmented by IFNγ + LPS stimulation (Fig. 7I). Importantly, these results implicate attenuated hypoxic gradients into the tumor core by the blockade of mitochondrial metabolism in $Nos2^{high}$ macrophages, thus increasing therapeutically targetable regions within the TME. Indeed, NO has been shown to enhance radiation sensitivity in hypoxic tumors [23,24].

3. Discussion

Macrophage-derived NO is a key mediator in the fight against tumor and pathogens as well as intercellular signaling and the modulation of immunometabolism [10]. Herein, we show that cytokine/LPS stimulated Nos2 expressing macrophages ($Nos2^{high}$) produce high NO flux due to the density of spatially distinct $Nos2^{high}$ expressing cells. This refutes the assumption of equal or homogenous distribution of Nos2 throughout the activated macrophage population and is consistent with feed-forward signaling shown in tumor cells [1]. Since NO impacts many cellular functions in a concentration-dependent manner, the extracellular NO flux that affects the immune response must be understood in terms of this single cell perspective as it provides insight into niches housing resistant tumor cells within the TME. Thus, extracellular flux of NO must be considered in terms, not only of the temporal response, but also spatial distribution. Mathematical modeling suggests

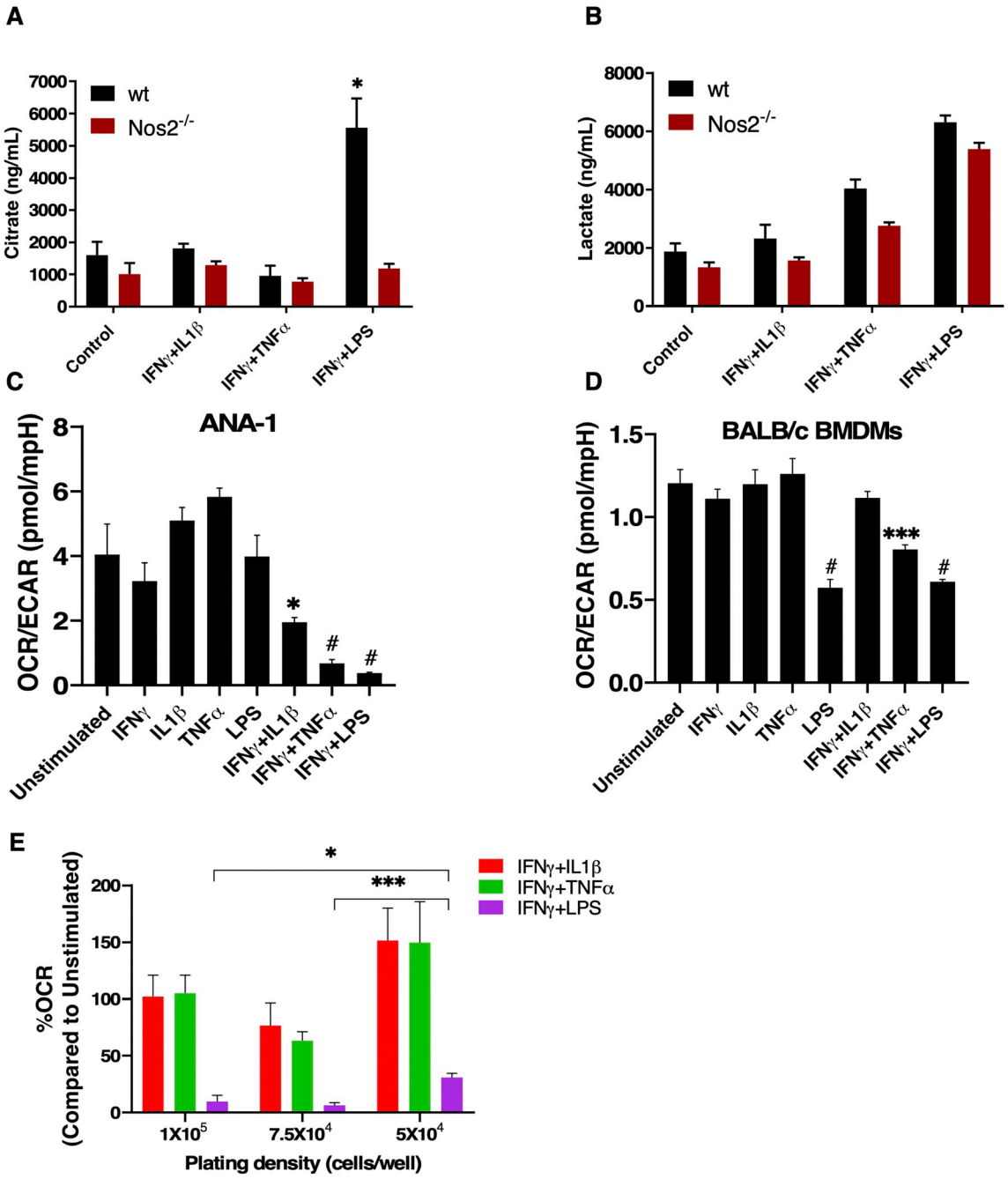

Fig. 6. Effects of NO on oxygen consumption are dependent on NO flux and frequency of Nos2+ cells. LC/MS analysis performed on cell lysates from 42h stimulated BALB/c BMDMs for measurement of citrate (A) and lactate (B) levels. OCR/ECAR in ANA-1 (C), and BALB/c (D) BMDMs stimulated with different combination stimuli for 18h. E. Change in % OCR of stimulated BMDMs compared to unstimulated cells at different plating densities. Error bars show SEM ($n \geq 3$).

that the extracellular NO generated from one Nos2 expressing cell is rapidly diluted through diffusion away from that cell. However, increased number of Nos2-expressing cells exponentially increased NO flux, which extended throughout the localized tissue region (Fig. 7B) [25]. This clustering of $Nos2^{high}$ cells creates neighborhoods in inflammatory tissue and tumors where NO levels are dramatically higher than that produced by a single cell. Thus, the spatial distribution of $Nos2^{high}$ cells will impact local effective NO flux and downstream effects.

A key observation of this study demonstrates the effect of Nos2-derived NO flux on OXPHOS both at the single cell level as well as neighboring cell. Previous studies revealed that NO regulates OXPHOS through inhibition of cytochrome c oxidase and by altering the mitochondrial membrane complexes by removal of iron from the Fe–S clusters [26,27]. Accumulation of citrate together with high citrulline, a product of Nos2, occurs at the higher density of cells corresponding to higher extracellular NO flux. As shown in Fig. S3B, inhibition of OXPHOS requires approximately 100–300 nM cellular NO, consistent with previous estimations of the $Nos2^{high}$ macrophage flux, a cellular flux 50–100 times higher than physiologic levels [10].

The regulation of OXPHOS by NO has critical implications in the tone of the immune response to cancer in both T cells and myeloid populations. Active OXPHOS in the immune system maintains macrophages and T-cells in an M2/T_h2 phenotype. In fact, OXPHOS reduction occurs in T_h1 cytotoxic effector T cells and M1 macrophages. Studies suggest that activated T cells increase NOS2 expression, which leads to

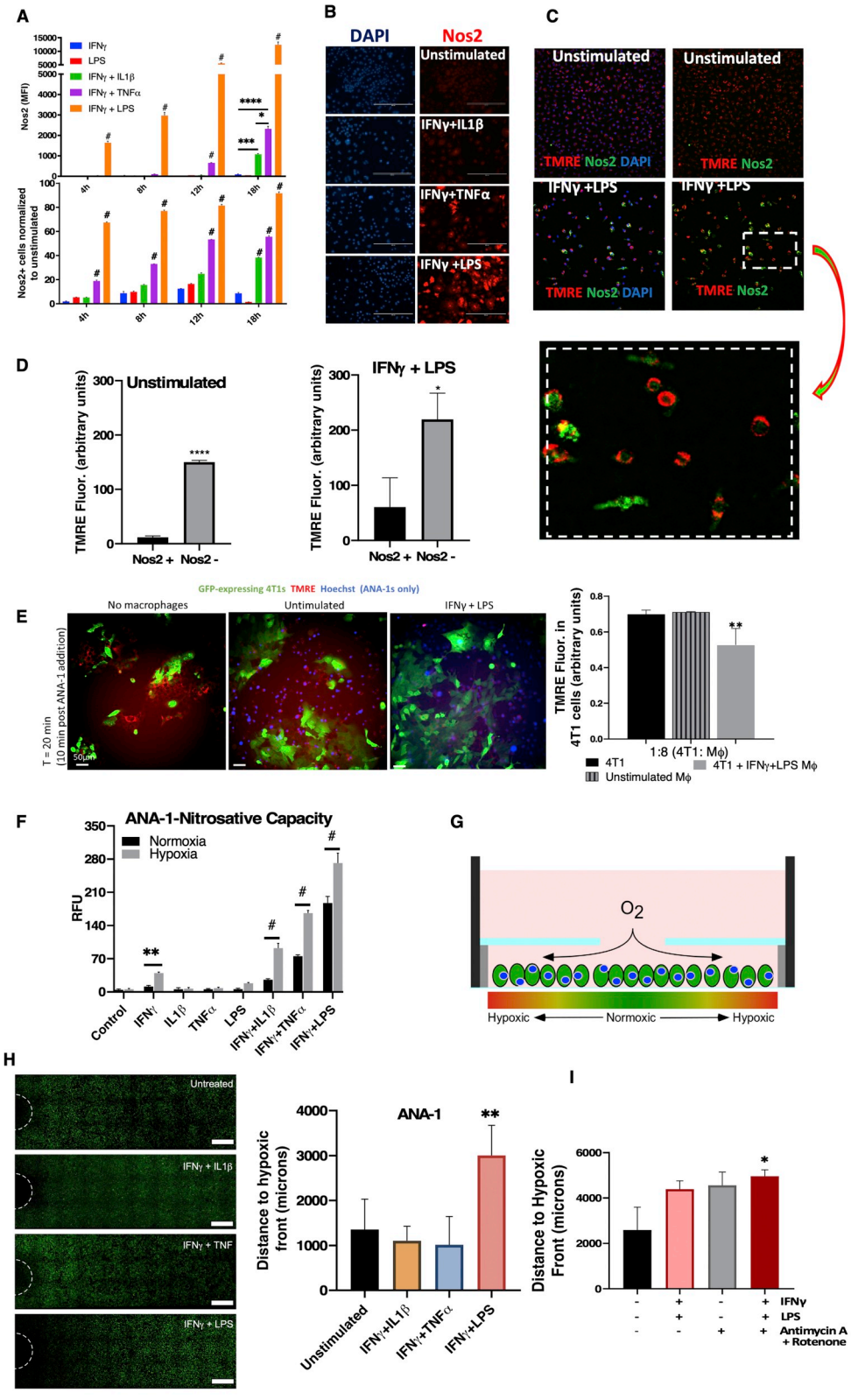

(caption on next page)

Fig. 7. Spatially distinct Nos2 expression affects single-cell redox immunometabolism. A. Flow cytometry analysis of numbers of Nos2+ cells and median Fluorescence intensity (MFI) values of Nos2 expression in stimulated ANA-1. Error bars show SEM, n > 3. B Microscopy analysis of Nos2+ cells in 18h stimulated ANA-1. C. IFNγ + LPS stimulated ANA-1 cells that were positive for TMRE (active mitochondria) [47] express low levels of Nos2. D. Statistical quantification of the red (TMRE) and green (Nos2) fluorescence intensities. Error bars show SD, n ≥ 3, scale bar = 200 μm. E. TMRE staining of 4T1-GFP cells cocultured with IFNγ + LPS stimulated ANA-1. Error bars show SD, n ≥ 3. F. Nitrosative capacity (DAN assay) of 18h stimulated ANA-1 under normoxia and hypoxia (3% O_2). G. Structure of REEC showing formation of hypoxic gradient. H. Distance to hypoxic front calculated from number of Image iT stained hypoxic, stimulated ANA-1 cells in the REECs as seen in the fluorescent microscope images. Scale bar = 500 μm. I. Image iT staining of hypoxic ANA-1 cells (stimulated or unstimulated) in the presence of antimycin A and rotenone in REECs. (For interpretation of the references to colour in this figure legend, the reader is referred to the Web version of this article.)

T cell exhaustion whereas NOS inhibition preserves memory T cells [28]. The production of IFNγ and TNFα by activated T-cells could stimulate macrophages to induce the $Nos2^{high}$ phenotype in a population of myeloid or tumor cells that tune the local immune response. This may in turn play an important role in tissue/tumor immunometabolism status of particular cellular neighborhoods. As shown here, elevated NO increases pO_2 which can affect the immune response [29]. Thus, Nos2 expression in the inflammatory microenvironment regulates the metabolic components of the immune response and pO_2, where the density of Nos2 expressing cells provide a tuning mechanism for the extent of the metabolic effects.

Immune cascades exhibit temporal components; high NO flux is essential for effective proinflammatory phenotype and transition to inflammation resolution. $Nos2^{high}$ macrophages can produce extracellular NO flux > 200 μM DETA/NO. This is relevant because IFNγ + LPS stimulated macrophages can generate this level of NO, which has been shown to induce the formation of T_{regs} capable of inhibiting IL17 and Th17 responses via IL10 induction [30]. Recently, autocrine IL10 from M1 macrophages was found to maintain the balance between inflammation and immunosuppression by dampening NO-mediated inhibition of OXPHOS [31]. Moreover, IFNγ + LPS stimulated macrophages can also activate TGFβ [11]. These findings suggest that Nos2 may be critical in the downregulation of inflammatory response in all leukocytes. For example, higher levels of NO from macrophages regulate major histocompatibility complex II (MHCII). While IFNγ, through the generation of reactive oxygen species, increases MHCII, the higher levels of NO induced through an antioxidant mechanism abates MHCII, therefore decreasing T_h1 polarization [32]. Thus, the spatial localization and level of NO is critical in the function of the immune response, regional NO levels, and local geometry of $Nos2^{high}$ cells could be key mediators of the onset of inflammatory versus immunosuppressive phenotypes within the TME.

There are two important features of stimulated macrophages, which include NO-independent induction of markers such CD86 and cytokine storm as well as NO-dependent features involving morphological changes that influence M1 functionality. While the induction of a proinflammatory cytokine storm in M1 macrophages is NO-independent, NO flux regulates cellular morphology where flattening of stimulated macrophages significantly distinguished their phenotype from that of unstimulated cells in a concentration dependent fashion. Studies have implied that macrophage cell shape with respect to M1 and M2 can dramatically affect the degree of polarization. For example, elongated macrophages (a M2 phenotype) may have Nos2 present but have considerably diminished capacity to release T_h1 cytokines compared to flattened/rounded cell shape. This indicates that cell shape plays a critical role in the degree of 'M1ness' and 'M2ness' and provides a tuning mechanism [17,33]. Further, this suggests a potential physiological impact in which IFNγ released from T cells/NK cells could prime macrophages, which migrate to infected or damaged areas, encounter higher levels of NO (from cells exposed to LPS or a cluster of $Nos2^{high}$ cells) promote morphological changes in these incoming macrophages that facilitate M1 functionality where they become more flattened and adhesive as opposed to rounded and less adhesive as shown in Fig. 3. A positive feedback loop can develop in which macrophages accumulate in an area of high NO and increase the density of $Nos2^{hi}$ cells thereby increasing M1 type responses. In addition, high NO flux in a local $Nos2^{hi}$ area would increase local pO_2, which may be important for T-cell proliferation and anti-pathogen or anti-tumor effects as well as transitioning to a wound-healing response [34,35]. Because macrophages will home to hypoxic areas, the increased NO may provide a method to increase pO_2 in the infected area. Thus, the $Nos2^{high}$ phenotype has important functional effects on macrophage morphological changes, regulation of OXPHOS, and decrease in IFNγ induced MHCII [32,36].

Activated M1 murine macrophages have increased levels of both Nos2 and Cox2, hinting at an important relationship between the two proteins in the inflammatory cascade. One important feature is that Cox2 and PGE2 are critical for M1 macrophages to sustain high levels of NO [37]. Here, we show that NO induces Cox2 expression and that Nos2 and Cox2 support their mutual expression and stabilization. This enables macrophages to sustain high NO flux, *i.e.* be NO tolerant, without undergoing apoptosis. Upon extended stimulation, the sustained high NO flux also augments Cox2. Interestingly, Nos2 and Cox2 are expressed in separate cells and regulate each other in a paracrine rather than autocrine fashion. The distinct expression of Nos2 and Cox2 in separate cells is also observed in tumor tissues from *in vivo* models. It is therefore insufficient to simply know the gross Nos2 and Cox2 expression levels. Thus, the interaction of Nos2 and Cox2 expressing cells, the proximity of $Nos2^{high}$ and $Cox2^{high}$ cells as well as the locations and phenotypes of other cells associated with these clustered populations may be critical in shaping the inflammatory microenvironment and immune response.

The expression of Nos2 and Cox2 in separate cells, can be explained in part by the earlier finding that IFNγ inhibits COX2 via STAT1 while inducing NOS2 in intestinal epithelial cells [38]. Furthermore, STAT1/3 inhibitors increase COX2 in macrophages both in humans and mouse models, suggesting that STAT1 phosphorylation has a role in inhibition of COX2 expression [39,40]. In contrast, IFNγ activation of STAT1 leads to increased NOS2 expression while inhibiting induction of COX2 [41]. TNFα and IL1β induce COX2 in most human and mouse cells [42,43]. The fact that Nos2 expression appears in only specific cell populations and Cox2 in others, may suggest a distribution of IFNγ sensitivity in the cell population. Increased Cox2 then leads to PGE2 production that supports Nos2 in a paracrine regulatory loop. Our previous studies showed that NOS2 and COX2 in humans are primarily expressed in tumor epithelium [2,8]. The current study extends our previous findings by showing that in the 4T1 tumor model, which closely resembles stage IV breast cancer, Nos2 and Cox2 tumor expression is spatially distinct in both tumor epithelium and macrophages. The stochastic model of M1 development predicts this would lead to separate cell populations expressing high levels of Nos2 and Cox2.

The interplay between NO in tumor cells and macrophages is an important determinant of cancer progression, treatment efficacy and the role of immune response [18] where $Nos2^{high}$ macrophages are proinflammatory while tumor Nos2 is immunosuppressive. Although increased macrophage Nos2 suggests a positive treatment response, NOS2 in the human tumor cells *in vivo* has been associated with poor outcome in many cancers. Importantly, NOS2 and NO have increased metastatic and increased invasiveness in response to 10–100 μM DETA/NO in both human and murine breast cancer cells. While elevated Nos2 in the macrophage had anticancer properties, the *trans* effect of NO demonstrated in this work suggests that NO produced from M1

macrophages could also induce migration and invasion of adjacent tumor cells. Indeed, 4T1 tumors in WT mice exhibited increased metastatic burden when compared to tumors in $Nos2^{-/-}$ mice, which implicates the involvement of immune cell Nos2 in metastatic spread. Moreover, pretreatment with Nos inhibitors before tumor injection curbed metastatic spread in 4T1 tumors [44]. Also, tumors in $Nos2^{-/-}$ mice treated with indomethacin grew slower and the median survival of these mice trended higher than their WT counterparts. Two $Nos2^{-/-}$ mice treated with indomethacin showed complete remission and did not relapse up to four months after removal of the treatment, which is indicative of immune involvement and not simply a direct inhibition of tumor cell proliferation by indomethacin. Importantly, these mice remained tumor-free two months after subsequent 4T1 tumor re-challenge. Furthermore, Nos2 and Cox2 expression was spatially distinct in tumor tissue as well, implicating the clinical importance of this paracrine relationship dramatically impacting prognosis through selection of aggressive tumor phenotypes in patients with ER- breast cancer [8]. Together these results support the use of the 4T1 model in studying NOS2/COX2 mechanisms as well as therapeutic efficacy of novel drugs.

4. Conclusions

In this report, we describe a new model highlighting the importance of localized NO flux in inflammatory response. We find that NO flux tunes the cellular response to inflammatory stimuli. Nos2-dependent and independent events collaborate to regulate proinflammatory macrophages. Autocrine, single cell effects on mitochondrial metabolism build up to cause paracrine effects including alleviation of hypoxia. Nos2 and Cox2 are expressed in different cells and cause paracrine regulation of one another. This forms another regulatory arm of the inflammatory response that could be exploited for therapy and prognosis as, $Nos2^{-/-}$ tumor bearing mice develop reduced lung metastasis compared to WT counterparts and indomethacin curbs primary tumor growth that was augmented in $Nos2^{-/-}$ mice. Importantly, the spatial distribution of $Nos2^{high}$ and $Cox2^{high}$ clusters within the tumor microenvironment could be exploited for therapeutically targeting aggressive populations localized to these regions. Thus, pretreatment with a Nos2 inhibitor followed by chemotherapy with inexpensive Cox inhibitors could potentially improve tumor immune response and may provide a therapeutic option for patients with aggressive triple negative breast cancer.

5. Materials and methods

5.1. Transwell migration assay

The ability of stimulated macrophages to induce migration of the aggressive 4T1 cells was studied using indirect coculture technique in a transwell chamber system. 4×10^5 ANA-1 cells were seeded into wells of a 24 well multidish, allowed to adhere for 3h and stimulated with IFNγ or a combination of IFNγ with IL1β, TNFα or LPS. After 6h, the stimulants were thoroughly washed off and cells were fed 10% DMEM containing 10 mM L-arginine. 50,000 4T1 cells in 100 μL serum-free media were seeded into the upper compartment of a 6.5 mm transwell insert of 8 μm pore size (Corning Inc., Costar™, #3422). The transwells were inserted into the ANA-1 containing wells and incubated at 37 °C/ 5%CO_2. After 20h the inserts were removed from the wells, non-migrated cells in the upper compartment were wiped off using cotton swabs and the inserts were then fixed for 30 min in 4% paraformaldehyde, stained in 1% crystal violet for 10min, washed in ultrapure water and viewed, and photographed using the Echo Revolve microscope. Nitrite levels in the spent media from the lower compartment was analyzed using Griess assay.

5.2. Metabolic analysis

Ability of mitochondria in stimulated macrophages to respond to stress was measured from the Oxygen consumption rate (OCR) and extracellular acidification rate (ECAR), that were examined using the XF96 Seahorse Metabolic Analyzer from Seahorse Biosciences. Briefly, cultured BMDMs as well as immortalized macrophages were plated at a seeding density of 1×10^5 cells/well in 200 μl of complete media except for the density experiments which were performed at seeding densities of 1×10^5, 7.5×10^4 and 5×10^4 cells/well. Metabolic mitochondrial stress tests were performed via manufacturer's protocol. OCR/ECAR ratios were calculated using the difference between first three determinations of basal OCR and the last three determinations of OCR and basal ECAR where indicated.

5.3. In vitro analysis using restricted exchange environment chambers

Restricted exchange environment chambers (REECs) were built with a 0.1 mm high, 18 mm in diameter stainless-steel O-ring glued to a 18 mm round coverslip with UV-curable epoxy. This was glued to a Mylar clamp that had been laser cut to fit the dimensions of the plate. The plates were prepared by gluing a lid to the rims of the wells to provide a small overhang of Mylar that the clamp could press against, giving the arms of the chamber a spring-force to keep the clamp air and water tight against the bottom of the plate. The lid was glued with UV-curable epoxy and the plate was sterilized in the UV Chamber. ANA-1 macrophages and murine BMDMs were plated at 75% confluency and adhered for 3 h. The cells were treated with cytokines for 18 h (ANA-1) or 24 h (BMDMs). For coculture experiments, stimulated ANA-1 cells were added onto an 18h culture of 4T1 cells at a ratio of 1 (4T1): 8 (ANA-1). For hypoxic gradient experiments, cells were dyed with 10 μM Image iT Hypoxia Reagent Green (ThermoFisher Scientific, Waltham, MA) for 30 min in the incubator. For studying the effects of inhibition of electron transport chain on hypoxia gradient, stimulated ANA-1 were also treated with 10 μM Antimycin A and 0.5 μM Rotenone (Mitochondrial Complex I inhibitors) at the same time as Image iT staining. Fresh media was added to the wells, and REECs were placed with sterilized forceps. Cells were imaged live after 2 h or every 15 min for 3 h (4T1-ANA-1 coculture experiments), on a Nikon TI-Eclipse microscope using a narrow band green filter at 20x and a heated stage insert. Images were stitched, and background and shading corrected in the Nikon software with a rolling ball radius of 5 μm and using shading correction images taken from Chroma slides. The cells were segmented in Imaris to determine their x,y coordinates with respect to the opening in the chamber and their fluorescence intensities. The Imaris statistics output was loaded into R Statistical Software and analyzed appropriately by average cell fluorescence vs. distance from center opening.

5.4. In vivo studies

The NCI-Frederick Animal Facility follows the Public Health Service Policy for the Care and Use of Laboratory Animals and is accredited by the Association for Accreditation of Laboratory Animal Care International and follows. Animal care was provided in accordance with the procedures outlined in the Guide for Care and Use of Laboratory Animals. For *in vivo* studies, female BALB/c mice obtained from the Frederick Cancer Research and Development Center Animal Production Area were housed five per cage. Eight to ten-week-old female BALB/c mice were injected with 2×10^5 4T1 cells in the fourth mammary fat pad. The tumor volume was measured by Vernier caliper and calculated as volume in cubic millimeters = $(\text{width}^2 \times \text{length})/2$. Eight days post tumor injection, 12 WT and 12 $Nos^{-/-}$ tumor bearing mice were started on 30 mg/L indomethacin in drinking water. Water was changed on alternate days and treatment was continued till the day the mice were euthanized. When the tumors reached 2000 mm^3, the mice were euthanized, tumors were collected for immunohistochemical analysis,

lungs were fixed in Bouin's solution and metastatic lesions were counted. Survival analysis was performed on indomethacin treated mice.

6. Statistical analysis

Statistical significance was ascertained using either Student *t*-test or one-way ANOVA with Tukey's multiple comparisons test. Data analysis was performed using GraphPad Prism 8 software, and significance is reported as *p ≤ 0.05, **p ≤ 0.01, ***p ≤ 0.001, #p≤0.0001. Imaris software was used to perform statistical analysis on fluorescent microscopic images as indicated in specific methods.

Declaration of competing interest

The authors have no competing interests to declare.

Acknowledgments

We gratefully acknowledge the contribution of the Pathology/Histotechnology Laboratory at NCI – Frederick. We immensely thank Timothy Back for extensive technical help and support during our animal experiments and collection of bones for preparation of macrophages. This work was supported by the NIH Intramural Research Programs Cancer and Inflammation Program (D.A.W., V.S., D.B., E.M.P, R.Y.S.C., L.A.R., G.A.B., and D.W.M.), Optical Microscopy and Image Analysis Laboratory (A.C.G., D.A.S., W.F.H., and S.J.L.). A.C.G was supported by the NIH Post-Baccalaureate Intramural Research Training Award Program at the National Cancer Institute. This project was funded in whole or in part with Federal funds from the National Cancer Institute, NIH, under Contract HHSN261200800001E. The content of this publication does not necessarily reflect the views or policies of the Department of Health and Human Services, nor does mention of trade names, commercial products, or organizations imply endorsement by the US Government.

Appendix A. Supplementary data

Supplementary data to this article can be found online at https://doi.org/10.1016/j.redox.2019.101354.

References

[1] J.L. Heinecke, L.A. Ridnour, R.Y. Cheng, C.H. Switzer, M.M. Lizardo, C. Khanna, S.A. Glynn, S.P. Hussain, H.A. Young, S. Ambs, D.A. Wink, Tumor microenvironment-based feed-forward regulation of NOS2 in breast cancer progression, Proceedings of the National Academy of Sciences of the United States of America, 2014.

[2] S.A. Glynn, B.J. Boersma, T.H. Dorsey, M. Yi, H.G. Yfantis, L.A. Ridnour, D.N. Martin, C.H. Switzer, R.S. Hudson, D.A. Wink, D.H. Lee, R.M. Stephens, S. Ambs, Increased NOS2 predicts poor survival in estrogen receptor-negative breast cancer patients, J. Clin. Investig. 120 (2010) 3843–3854.

[3] L.A. Ridnour, A.N. Windhausen, J.S. Isenberg, N. Yeung, D.D. Thomas, M.P. Vitek, D.D. Roberts, D.A. Wink, Nitric oxide regulates matrix metalloproteinase-9 activity by guanylyl-cyclase-dependent and -independent pathways, Proc. Natl. Acad. Sci. U. S. A. 104 (2007) 16898–16903.

[4] L.A. Ridnour, J.S. Isenberg, M.G. Espey, D.D. Thomas, D.D. Roberts, D.A. Wink, Nitric oxide regulates angiogenesis through a functional switch involving thrombospondin-1, Proc. Natl. Acad. Sci. U. S. A. 102 (2005) 13147–13152.

[5] M.G. Espey, K.M. Miranda, R.M. Pluta, D.A. Wink, Nitrosative capacity of macrophages is dependent on nitric-oxide synthase induction signals, J. Biol. Chem. 275 (2000) 11341–11347.

[6] D.C. Hinshaw, L.A. Shevde, The Tumor Microenvironment Innately Modulates Cancer Progression, Cancer Res, 2019.

[7] S. Granados-Principal, Y. Liu, M.L. Guevara, E. Blanco, D.S. Choi, W. Qian, T. Patel, A.A. Rodriguez, J. Cusimano, H.L. Weiss, H. Zhao, M.D. Landis, B. Dave, S.S. Gross, J.C. Chang, Inhibition of iNOS as a novel effective targeted therapy against triple-negative breast cancer, Breast Cancer Res. 17 (2015) 25.

[8] D. Basudhar, S.A. Glynn, M. Greer, V. Somasundaram, J.H. No, D.A. Scheiblin, P. Garrido, W.F. Heinz, A.E. Ryan, J.M. Weiss, R.Y.S. Cheng, L.A. Ridnour, S.J. Lockett, D.W. McVicar, S. Ambs, D.A. Wink, Coexpression of NOS2 and COX2 accelerates tumor growth and reduces survival in estrogen receptor-negative breast cancer, Proc Natl Acad Sci U S A, 2017.

[9] J. Gunzle, N. Osterberg, J.E. Saavedra, A. Weyerbrock, Nitric oxide released from JS-K induces cell death by mitotic catastrophe as part of necrosis in glioblastoma multiforme, Cell Death Dis. 7 (2016) e2349.

[10] D.D. Thomas, J.L. Heinecke, L.A. Ridnour, R.Y. Cheng, A.H. Kesarwala, C.H. Switzer, D.W. McVicar, D.D. Roberts, S. Glynn, J.M. Fukuto, D.A. Wink, K.M. Miranda, Signaling and stress: the redox landscape in NOS2 biology, Free Radical Biol. Med. 87 (2015) 204–225.

[11] Y. Vodovotz, L. Chesler, H. Chong, S.J. Kim, J.T. Simpson, W. DeGraff, G.W. Cox, A.B. Roberts, D.A. Wink, M.H. Barcellos-Hoff, Regulation of transforming growth factor beta1 by nitric oxide, Cancer Res. 59 (1999) 2142–2149.

[12] F. Klug, H. Prakash, P.E. Huber, T. Seibel, N. Bender, N. Halama, C. Pfirschke, R.H. Voss, C. Timke, L. Umansky, K. Klapproth, K. Schakel, N. Garbi, D. Jager, J. Weitz, H. Schmitz-Winnenthal, G.J. Hammerling, P. Beckhove, Low-dose irradiation programs macrophage differentiation to an iNOS(+)/M1 phenotype that orchestrates effective T cell immunotherapy, Cancer Cell 24 (2013) 589–602.

[13] I.M. Sektioglu, R. Carretero, N. Bender, C. Bogdan, N. Garbi, V. Umansky, L. Umansky, K. Urban, M. von Knebel-Doberitz, V. Somasundaram, D. Wink, P. Beckhove, G.J. Hammerling, Macrophage-derived nitric oxide initiates T-cell diapedesis and tumor rejection, OncoImmunology 5 (2016) e1204506.

[14] B.A. Pulaski, S. Ostrand-Rosenberg, Mouse 4T1 breast tumor model, Curr Protoc Immunol Chapter 20 (2001) Unit 20 2.

[15] Z. Mi, H. Guo, P.Y. Wai, C. Gao, J. Wei, P.C. Kuo, Differential osteopontin expression in phenotypically distinct subclones of murine breast cancer cells mediates metastatic behavior, J. Biol. Chem. 279 (2004) 46659–46667.

[16] C.J. Aslakson, F.R. Miller, Selective events in the metastatic process defined by analysis of the sequential dissemination of subpopulations of a mouse mammary tumor, Cancer Res. 52 (1992) 1399–1405.

[17] F.Y. McWhorter, T. Wang, P. Nguyen, T. Chung, W.F. Liu, Modulation of macrophage phenotype by cell shape, Proc. Natl. Acad. Sci. U. S. A. 110 (2013) 17253–17258.

[18] B. Brune, N. Courtial, N. Dehne, S.N. Syed, A. Weigert, Macrophage NOS2 in tumor leukocytes, Antioxidants Redox Signal. 26 (2017) 1023–1043.

[19] M.Y. Janssens, D.L. Van den Berge, V.N. Verovski, C. Monsaert, G.A. Storme, Activation of inducible nitric oxide synthase results in nitric oxide-mediated radiosensitization of hypoxic EMT-6 tumor cells, Cancer Res. 58 (1998) 5646–5648.

[20] H. Jiang, M. De Ridder, V.N. Verovski, P. Sonveaux, B.F. Jordan, K. Law, C. Monsaert, D.L. Van den Berge, D. Verellen, O. Feron, B. Gallez, G.A. Storme, Activated macrophages as a novel determinant of tumor cell radioresponse: the role of nitric oxide-mediated inhibition of cellular respiration and oxygen sparing, Int. J. Radiat. Oncol. Biol. Phys. 76 (2010) 1520–1527.

[21] D.D. Thomas, Breathing new life into nitric oxide signaling: a brief overview of the interplay between oxygen and nitric oxide, Redox Biol 5 (2015) 225–233.

[22] J.H. Hoh, J.L. Werbin, W.F. Heinz, Restricted exchange microenvironments for cell culture, Biotechniques 64 (2018) 101–109.

[23] M. Nagane, H. Yasui, T. Yamamori, S. Zhao, Y. Kuge, N. Tamaki, H. Kameya, H. Nakamura, H. Fujii, O. Inanami, Radiation-induced nitric oxide mitigates tumor hypoxia and radioresistance in a murine SCCVII tumor model, Biochem. Biophys. Res. Commun. 437 (2013) 420–425.

[24] P. Howard-Flanders, Effect of nitric oxide on the radiosensitivity of bacteria, Nature 180 (1957) 1191–1192.

[25] J.R. Lancaster Jr., Simulation of the diffusion and reaction of endogenously produced nitric oxide, Proc. Natl. Acad. Sci. U. S. A. 91 (1994) 8137–8141.

[26] G.C. Brown, Nitric oxide and mitochondrial respiration, Biochim. Biophys. Acta 1411 (1999) 351–369.

[27] J.B. Hibbs Jr., R.R. Taintor, Z. Vavrin, E.M. Rachlin, Nitric oxide: a cytotoxic activated macrophage effector molecule, Biochem. Biophys. Res. Commun. 157 (1988) 87–94.

[28] M. Vig, S. Srivastava, U. Kandpal, H. Sade, V. Lewis, A. Sarin, A. George, V. Bal, J.M. Durdik, S. Rath, Inducible nitric oxide synthase in T cells regulates T cell death and immune memory, J. Clin. Investig. 113 (2004) 1734–1742.

[29] C.T. Lee, T. Mace, E.A. Repasky, Hypoxia-driven immunosuppression: a new reason to use thermal therapy in the treatment of cancer? Int. J. Hyperth. 26 (2010) 232–246.

[30] W. Niedbala, A.G. Besnard, H.R. Jiang, J.C. Alves-Filho, S.Y. Fukada, D. Nascimento, A. Mitani, P. Pushparaj, M.H. Alqahtani, F.Y. Liew, Nitric oxide-induced regulatory T cells inhibit Th17 but not Th1 cell differentiation and function, J. Immunol. 191 (2013) 164–170.

[31] W.A. Baseler, L.C. Davies, L. Quigley, L.A. Ridnour, J.M. Weiss, S.P. Hussain, D.A. Wink, D.W. McVicar, Autocrine IL-10 functions as a rheostat for M1 macrophage glycolytic commitment by tuning nitric oxide production, Redox Biol 10 (2016) 12–23.

[32] O. Harari, J.K. Liao, Inhibition of MHC II gene transcription by nitric oxide and antioxidants, Curr. Pharmaceut. Des. 10 (2004) 893–898.

[33] F.Y. McWhorter, C.T. Davis, W.F. Liu, Physical and mechanical regulation of macrophage phenotype and function, Cell. Mol. Life Sci. 72 (2015) 1303–1316.

[34] E.N. McNamee, D. Korns Johnson, D. Homann, E.T. Clambey, Hypoxia and hypoxia-inducible factors as regulators of T cell development, differentiation, and function, Immunol. Res. 55 (2013) 58–70.

[35] C.K. Sen, Wound healing essentials: let there be oxygen, Wound Repair Regen. 17 (2009) 1–18.

[36] J. Xaus, M. Comalada, M. Barrachina, C. Herrero, E. Gonalons, C. Soler, J. Lloberas, A. Celada, The expression of MHC class II genes in macrophages is cell cycle dependent, J. Immunol. 165 (2000) 6364–6371.

[37] A. von Knethen, B. Brune, Attenuation of macrophage apoptosis by the cAMP-signaling system, Mol. Cell. Biochem. 212 (2000) 35–43.

[38] K.L. Wright, S.A. Weaver, K. Patel, K. Coopman, M. Feeney, G. Kolios, D.A. Robertson, S.G. Ward, Differential regulation of prostaglandin E biosynthesis by interferon-gamma in colonic epithelial cells, Br. J. Pharmacol. 141 (2004) 1091–1097.

[39] J.C. Chen, K.C. Huang, B. Wingerd, W.T. Wu, W.W. Lin, HMG-CoA reductase inhibitors induce COX-2 gene expression in murine macrophages: role of MAPK cascades and promoter elements for CREB and C/EBPbeta, Exp. Cell Res. 301 (2004) 305–319.

[40] A. Habib, I. Shamseddeen, M.S. Nasrallah, T.A. Antoun, G. Nemer, J. Bertoglio, R. Badreddine, K.F. Badr, Modulation of COX-2 expression by statins in human monocytic cells, FASEB J. 21 (2007) 1665–1674.

[41] J. Gao, D.C. Morrison, T.J. Parmely, S.W. Russell, W.J. Murphy, An interferon-gamma-activated site (GAS) is necessary for full expression of the mouse iNOS gene in response to interferon-gamma and lipopolysaccharide, J. Biol. Chem. 272 (1997) 1226–1230.

[42] P.S. Biswas, K. Banerjee, B. Kim, P.R. Kinchington, B.T. Rouse, Role of inflammatory cytokine-induced cyclooxygenase 2 in the ocular immunopathologic disease herpetic stromal keratitis, J. Virol. 79 (2005) 10589–10600.

[43] T. Kuwano, S. Nakao, H. Yamamoto, M. Tsuneyoshi, T. Yamamoto, M. Kuwano, M. Ono, Cyclooxygenase 2 is a key enzyme for inflammatory cytokine-induced angiogenesis, FASEB J. 18 (2004) 300–310.

[44] A. Kij, K. Kus, M. Smeda, A. Zakrzewska, B. Proniewski, K. Matyjaszczyk, A. Jasztal, M. Stojak, M. Walczak, S. Chlopicki, Differential effects of nitric oxide deficiency on primary tumour growth, pulmonary metastasis and prostacyclin/thromboxane A2 balance in orthotopic and intravenous murine models of 4T1 breast cancer, J. Physiol. Pharmacol. 69 (2018).

[45] A.M. Miles, D.A. Wink, J.C. Cook, M.B. Grisham, Determination of nitric oxide using fluorescence spectroscopy, Methods Enzymol. 268 (1996) 105–120.

[46] K.M. Miranda, M.G. Espey, D.A. Wink, A rapid, simple spectrophotometric method for simultaneous detection of nitrate and nitrite, Nitric Oxide 5 (2001) 62–71.

[47] L.C. Crowley, M.E. Christensen, N.J. Waterhouse, Measuring mitochondrial transmembrane potential by TMRE staining, Cold Spring Harb. Protoc. 12 (2016) 1092–1096.

[49] L.A. Ridnour, R.Y. Cheng, J.M. Weiss, S. Kaur, D.R. Soto-Pantoja, D. Basudhar, J.L. Heinecke, C.A. Stewart, W. DeGraff, A.L. Sowers, A. Thetford, A.H. Kesarwala, D.D. Roberts, H.A. Young, J.B. Mitchell, G. Trinchieri, R.H. Wiltrout, D.A. Wink, NOS inhibition modulates immune polarization and improves radiation-induced tumor growth delay, Cancer Res. 75 (2015) 2788–2799.